Sensitive and accurate determination of REEs by highly-efficiency miniaturized ultrasonic nebulization sampling system coupled with inductively coupled plasma mass spectrometry

Junhang Dong,[1,2,#] Meihua Chen[3,#], Lujie Li,[1,2] Pengju Xing,[1] Shuyang Li,[1] Zhe Zhang,[1] Jingwen Zhang,[1] Jinzhao Liu,[2] Xing Liu,[1] Wenkai Zhang[1,2], Huan Tian,[2] Hongtao Zheng[2] and Zhenli Zhu,[1,2,4*].

[1] State Key Laboratory of Biogeology and Environmental Geology, School of Earth Sciences, China University of Geosciences, Wuhan 430074, China

[2] Faculty of Material Science and Chemistry, China University of Geosciences, Wuhan 430074, China

[3] Changsha Natural Resources Comprehensive Survey Center, Changsha 410000, China

[4] Hubei Key Laboratory of Yangtze Catchment Environmental Aquatic Science, Wuhan, 430078, China

Correspondence and requests for materials should be addressed to:
Dr. Zhenli Zhu, State Key Laboratory of Biogeology and Environmental Geology, China University of Geosciences, Wuhan 430074, China, Email: zlzhu@cug.edu.cn

Table of Contents

Figure S-3 The calibration curve of REEs in MUN-ICP-MS with the low REEs concentrations ranging from 0.03 to 0.30 ng mL^{-1} and high REEs concentrations ranging from 1 to 20 ng mL^{-1}.

Figure S-4 The reproducibility of REEs signal intensities measured at the concentration of (a) 1 ng mL^{-1} and (b) 10 ng mL^{-1} by MUN-ICP-MS (N = 8).

Figure S-5 The comparison of the Gd measured values of GSD-10, GSS-7, GSS-9, GSS-12, BCR-2, and BHVO-2 using the MUN-ICP-MS by choosing the ^{157}Gd without any correction and the ^{160}Gd with the mathematical correction.

Table S-1 Instrumental operating conditions and data acquisition parameters for PN-ICP-MS and MUN-ICP-MS.

Table S-2 Analysis and rinsing process settings for MUN-ICP-MS.

Table S-3 Comparison of sample introduction efficiency (η) with different MUN nebulization rate.

Table S-4 The voltage of square waveform of MUN selected at different duty ratios.

Table S-5 Measurement results (N = 3) of REEs mass fractions in two sediments (GSD-10, GSS-9) and two soils (GSS-7, GSS-12) CRMs using the MUN-ICP-MS.

Table S-6 Measurement results (N = 3) of REEs mass fractions in two basalt CRMs (BCR-2 and BHVO-2) using the MUN-ICP-MS.

Reference.

Section 1. The setup of the MUN unit.

The MUN sheet is connected with the spray chamber by using an O-ring (i.d. 10 mm, o.d. 16 mm) with super glue (3M). A peristaltic pump that comes with the ICP-MS instrument provides the introduction of sample solution with a pump tube (i.d. 0.25 mm). The front end of the pump tube is connected with a PFA capillary (i.d. 0.1 mm), and the rear end is connected to a quartz capillary (i.d. 30 μm), which is kept horizontal and the outlet of the quartz capillary located above the central area of the MUN with a very short interval of about 0.1 mm. The capillary was positioned horizontally, which forms an angle of 90° to the surface of the MUN. Under operation, liquid was allowed to flow onto the central area of transducer, where nebulization occurred.

Section 2. High-pressure bomb sample digestion process.

For the four sediments and soils CRMs standard samples, 100 mg of samples powder were precisely weighed into a PTFE-lined stainless-steel bomb, and then 1.0 mL concentrated HNO_3 and 1.0 mL HF were slowly added. Digestion blank was also set for digestion process. After that, the bombs were sealed and heated to 190℃ in an electric oven for 48 hours to ensure complete digestion. After cooling, the bombs were opened and placed on a hotplate to evaporate the sample solutions at 100℃. Then, 1 mL concentration HNO_3 was added and evaporated to dryness at 100℃ in order to remove HF. After that, 3 mL 30% HNO_3 was added, and the bombs were sealed again and heated in an oven at 190℃ for 12 hours. After cooling, the bombs were opened and the solutions were transferred to PFA beakers. These beakers were placed on a hotplate at 100℃ to evaporate the sample solutions. Then, 0.5 mL DI-water was added and evaporated to dryness at 100℃ again in order to remove HNO_3 completely and redissolved in 8 mL 2% HNO_3.

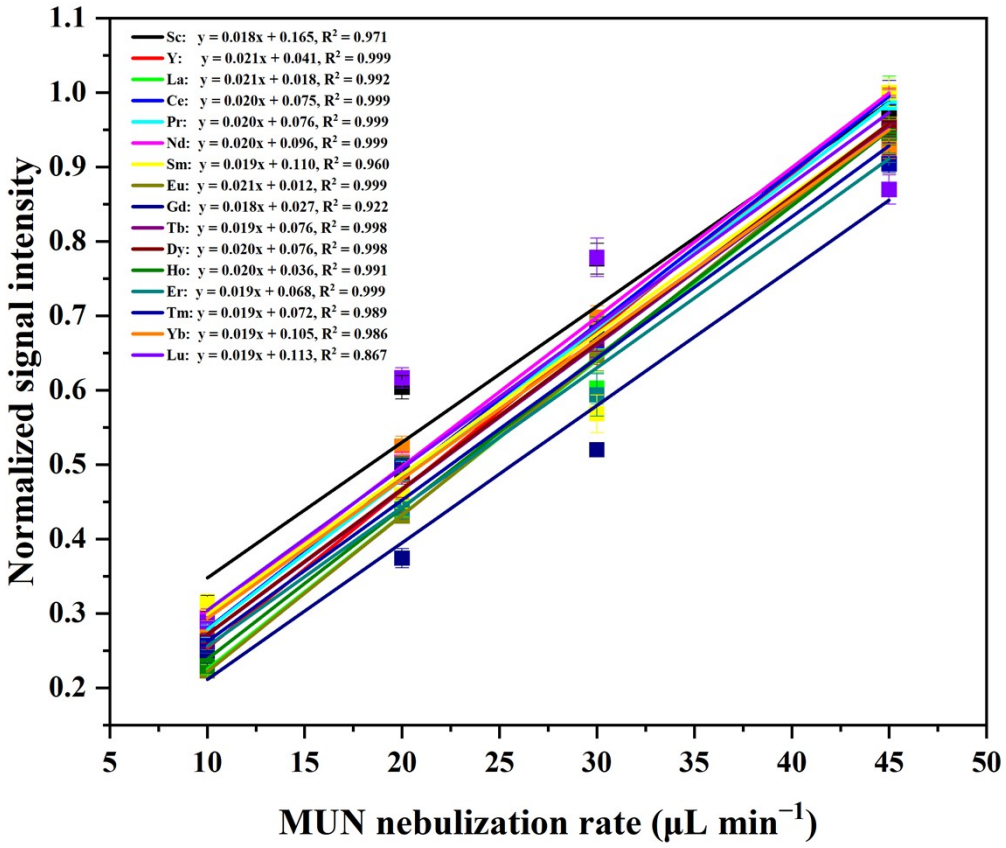

Figure S-1. The linear fit equations of the normalized signal intensities of REEs using MUN-ICP-MS with the nebulization rate increasing from 10 to 45 μL min^{-1}. The signal intensities of REEs are independently normalized by maximum value. Each point is the average from six measurements (n = 6) with the error bars defined as ± SD.

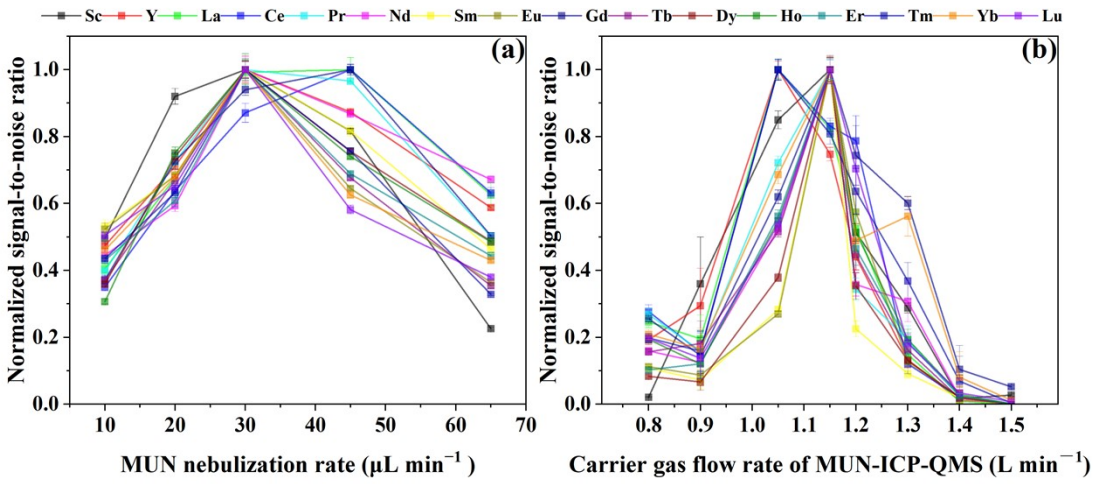

Figure S-2. (a) Normalized signal-to-noise ratios of 16 REEs with different nebulization rate of MUN under the optimal conditions obtained by auto-tune, respectively. (b) Optimization of Ar carrier gas flow rate with the MUN nebulization rate of 30 μL min^{-1}. Square waveform with duty ratio of 50% was set for MUN. (Signal-to-noise ratios of REEs are independently normalized by maximum value, each point is the average from six measurements (n = 6) with the error bars defined as ± SD)

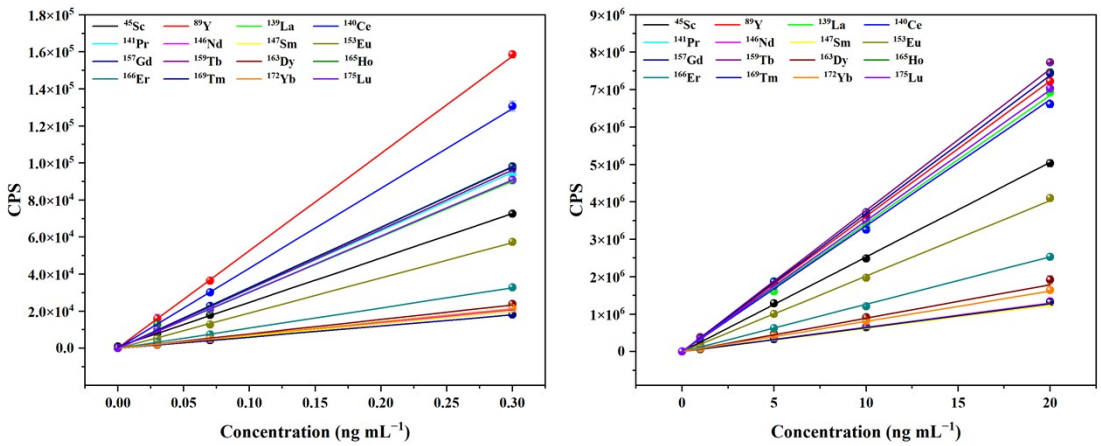

Figure S-3 Calibration curve of REEs in MUN-ICP-MS with the low REEs concentrations ranging from 0.03 to 0.30 ng mL^{-1} and high REEs concentrations ranging from 1 to 20 ng mL^{-1}. Each point is the average from 3 measurements (n = 3) with the error bars defined as ± SD.

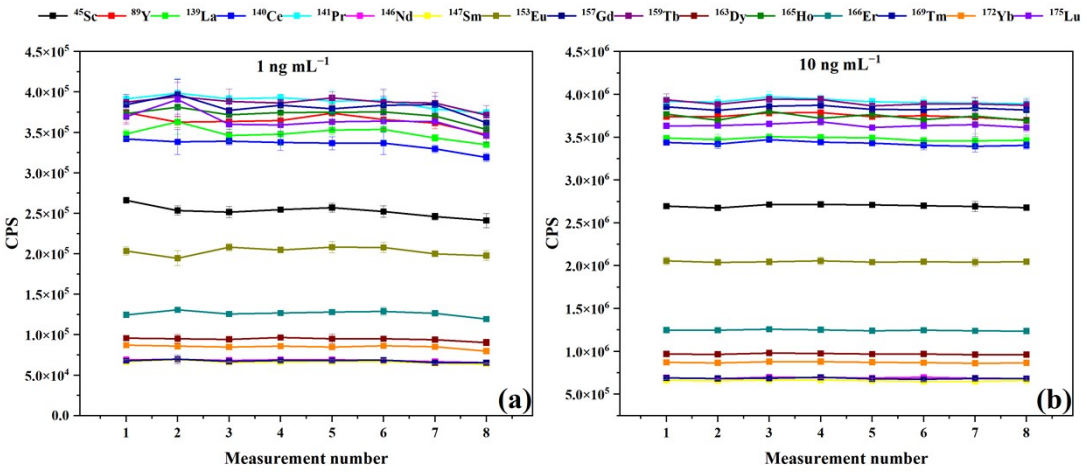

Figure S-4 The reproducibility of REEs signal intensities measured at the concentration of (a) 1 ng mL^{-1} and (b) 10 ng mL^{-1} by MUN-ICP-MS (N = 8). (Each point is the average intensity within a single analysis time and the error bars are defined as the internal precision of a single analysis)

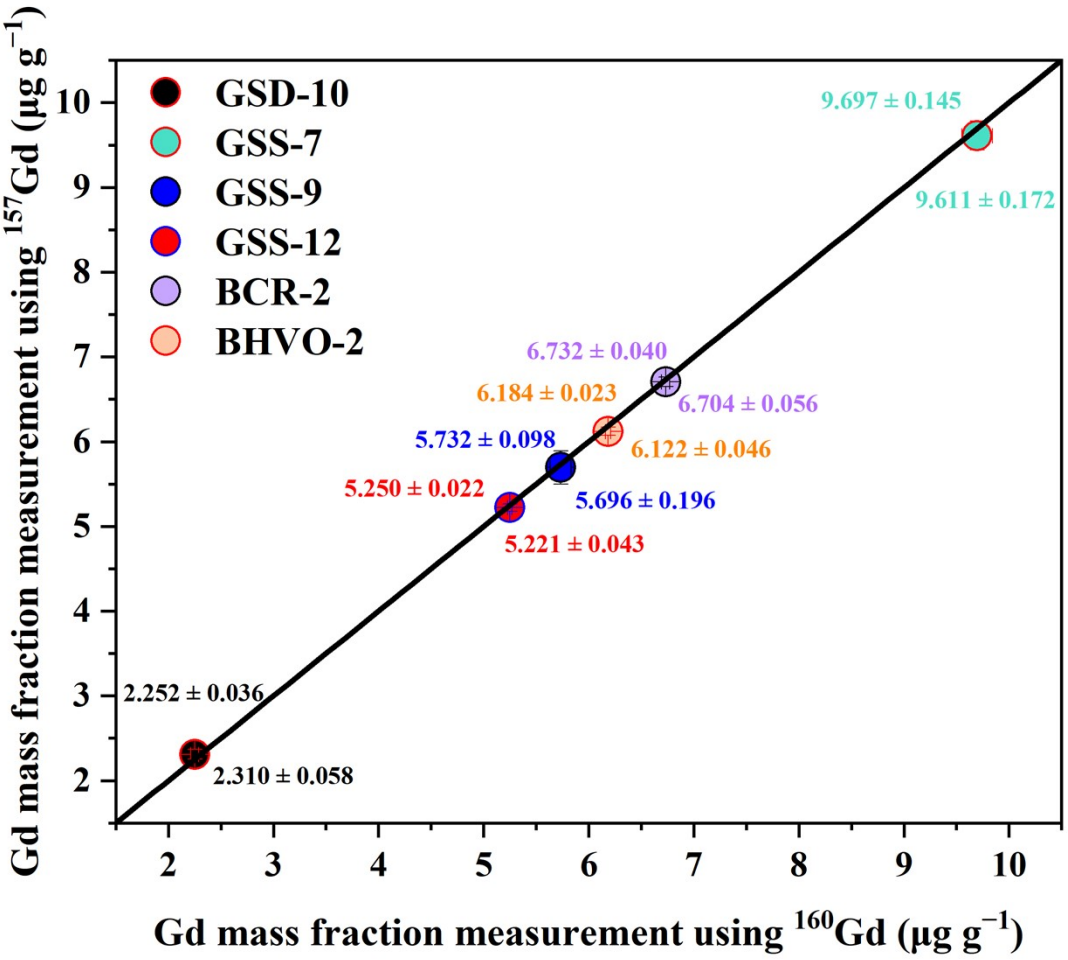

Figure S-5 The comparison of the Gd measured values of GSD-10, GSS-7, GSS-9, GSS-12, BCR-2, and BHVO-2 using the MUN-ICP-MS by choosing the ^{157}Gd without any correction and the ^{160}Gd with the mathematical correction (Mc (160) = M (160) * 1 – M (163) * 0.09357). Each point is the average from 3 measurements (n = 3) with the error bars defined as ± SD.

Table S-1 Instrumental operating conditions and data acquisition parameters for PN-ICP-MS and MUN-ICP-MS.

Parameter	PN-ICP-MS	MUN-ICP-MS
Plasma power (W)	1550	
Plasma gas (L min^{-1})	15.0	
Auxiliary gas (L min^{-1})	0.9	
Sampling depth (mm)	8.0	
Interface cones	Nickel	
Extract 1 (V)	20.0	
Extract 2 (V)	-90	
Omega Bias (V)	-90	
Omega Lens (V)	8.0	
Cell Entrance (V)	-30	
Cell Exit (V)	-50	
Deflect (V)	15.4	
Plate Bias (V)	-35	
He flow rate (mL min^{-1})	CRC activated: 2 CRC inactivated: 0	
Octp Bias (V)	-8.0	
Octp RF (V)	200	
Energy Discrimination (V)	5.0	
Monitored isotopes	^{89}Y, ^{139}La, ^{140}Ce, ^{141}Pr, ^{146}Nd, ^{147}Sm, ^{153}Eu, ^{157}Gd, ^{159}Tb, ^{163}Dy, ^{165}Ho, ^{166}Er, ^{169}Tm, ^{172}Yb, ^{175}Lu	
Signal processing	3 points per peak	
Sweep	100	
Integration time (s)	0.1	
Replicates	3	
Nebulizer	MicroMist (340 µL min^{-1})	MUN (30 µL min^{-1})
Carrier Gas (L min^{-1})	1.10	1.15
Analysis time (s)	30	30

Table S-2. Analysis and rinsing process settings for MUN-ICP-MS.

Step	Operation settings	Time (s)
1	MUN: stop; Sample solution uptake: 60 μL min^{-1} (Sample solution)	2
2	MUN: 0.11 W (30 μL min^{-1}); Sample solution uptake: 30 μL min^{-1} (Sample solution)	30
3	MUN: 0.11 W (30 μL min^{-1}); Sample solution uptake: stop	8
4	MUN: 0.11 W (30 μL min^{-1}); Sample solution uptake: 30 μL min^{-1} (UPW)	15
5	MUN: 0.11 W (30 μL min^{-1}); Sample solution uptake: Stop	2

Table S-3. Comparison of sample introduction efficiency (η) with different MUN nebulization rate.

Nebulization rate of MUN (μL min^{-1})	**MUN power (W)**	**Running time (min)**	**Feed (g)**	**Chamber weight before sampling (g)**	**Chamber weight after sampling (g)**	**Waste (g)**	**η**
10	0.05	30	0.321	13.228	13.228	/	100%
	0.05	60	0.629	13.228	13.228	/	100%
20	0.08	30	0.624	13.228	13.228	/	100%
	0.08	60	1.298	13.228	13.228	/	100%
30	0.11	30	0.925	13.228	13.228	/	100%
	0.11	60	1.782	13.228	13.228	/	100%
45	0.15	5	0.233	13.228	13.299	0.024	89.7%
	0.15	5	0.231	13.228	13.293	0.022	90.3%
65	0.22	5	0.330	13.228	13.397	0.070	78.9%
	0.22	5	0.337	13.228	13.399	0.064	81.1%

Table S-4 The voltage of square waveform of MUN selected at different duty ratios.

Duty ratio/%	**voltage/V**
20	15.2
30	14.0
40	12.6
50	12.4
60	12.0
80	11.8

Table S-5 Measured results (N = 3) of REEs mass fractions in two sediments (GSD-10, GSS-9) and two soils (GSS-7, GSS-12) CRMs using the MUN-ICP-MS. The measured values are the average from 3 measurements (n = 3) by MUN-ICP-MS with the uncertainties error bars defined as ± SD.

Element	GSD-10 (μg g^{-1})			GSS-7 (μg g^{-1})			GSS-9 (μg g^{-1})		GSS-12 (μg g^{-1})	
	Measured*	Certified[#1]	Recommended[&1]	Measured*	Certified[#]	Recommended[&1]	Measured*	Recommended[&2]	Measured*	Recommended[&3]
Sc	3.92 ± 0.07	3.22 ± 0.14	4.1 ± 0.4	26.93 ± 0.24	26.5 ± 0.1	28.0 ± 2.0	12.21 ± 0.22	12 ± 2	12.49 ± 0.37	12.6 ± 0.4
Y	13.64 ± 0.11	13.4 ± 0.5	14.0 ± 2.0	28.16 ± 0.04	28.8 ± 0.8	27.0 ± 4.0	25.74 ± 0.13	25.0 ± 2.0	26.87 ± 0.16	26.4 ± 0.9
La	12.23 ± 0.13	12.1 ± 0.3	13.0 ± 0.9	45.14 ± 0.19	46.1 ± 0.9	46.0 ± 5.0	38.87 ± 0.23	38.0 ± 3.0	30.01 ± 0.23	29.0 ± 2.0
Ce	37.13 ± 0.33	37.4 ± 0.6	38 ± 4.0	105.69 ± 0.57	104.0 ± 1.0	98.0 ± 11.0	73.71 ± 0.38	74.0 ± 4.0	56.66 ± 0.20	57.0 ± 2.0
Pr	2.897 ± 0.050	2.91 ± 0.09	3.2 ± 0.4	10.94 ± 0.21	11.4 ± 0.2	11.0 ± 1.0	8.333 ± 0.095	8.5 ± 0.7	6.881 ± 0.048	7.0 ± 0.4
Nd	10.98 ± 0.24	10.8 ± 0.3	11.8 ± 1.1	43.77 ± 0.26	44.8 ± 1.0	45.0 ± 2.0	32.07 ± 0.31	32.0 ± 3.0	27.17 ± 0.36	27.9 ± 1.2
Sm	2.348 ± 0.026	2.33 ± 0.01	2.4 ± 0.2	9.847 ± 0.182	10.3 ± 0.1	10.3 ± 0.4	6.224 ± 0.159	6.2 ± 0.5	5.770 ± 0.136	5.6 ± 0.4
Eu	0.4544 ± 0.0069	0.45 ± 0.02	0.47 ± 0.04	3.453 ± 0.043	3.41 ± 0.04	3.40 ± 0.20	1.273 ± 0.008	1.27 ± 0.11	1.245 ± 0.018	1.22 ± 0.04
Gd	2.252 ± 0.036	2.17 ± 0.09	2.2 ± 0.2	9.697 ± 0.145	9.25 ± 0.12	9.6 ± 0.9	5.732 ± 0.098	5.4 ± 0.6	5.250 ± 0.022	5.1 ± 0.3
Tb	0.3589 ± 0.0024	0.36 ± 0.01	0.42 ± 0.1	1.310 ± 0.037	1.35 ± 0.01	1.30 ± 0.20	0.8756 ± 0.0077	0.86 ± 0.12	0.8504 ± 0.0188	0.84 ± 0.06
Dy	2.198 ± 0.042	2.18 ± 0.12	2.2 ± 0.3	6.581 ± 0.037	6.37 ± 0.21	6.6 ± 0.6	4.754 ± 0.101	4.7 ± 0.4	4.927± 0.033	4.9 ± 0.3
Ho	0.4469 ± 0.0046	0.45 ± 0.01	0.45 ± 0.07	1.151 ± 0.018	1.11 ± 0.03	1.10 ± 0.20	1.021 ± 0.005	1.03 ± 0.07	1.015 ± 0.010	1.01 ± 0.04
Er	1.279 ± 0.032	1.29 ± 0.09	1.3 ± 0.2	2.852 ± 0.073	2.57 ± 0.10	2.7 ± 0.5	2.881 ± 0.023	2.8 ± 0.3	2.971 ± 0.050	2.9 ± 0.2
Tm	0.1883 ± 0.0040	0.19 ± 0.01	0.20 ± 0.03	0.3941 ± 0.0091	0.38 ± 0.02	0.42 ± 0.05	0.435 ± 0.007	0.42 ± 0.06	0.4577 ± 0.0089	0.44 ± 0.05
Yb	1.198 ± 0.027	1.21 ± 0.07	1.2 ± 0.2	2.343 ± 0.026	2.22 ± 0.04	2.4 ± 0.4	2.570 ± 0.014	2.6 ± 0.4	3.022 ± 0.046	2.9 ± 0.2
Lu	0.1755 ± 0.0033	0.18 ± 0.01	0.19 ± 0.03	0.3435 ± 0.0098	0.32 ± 0.01	0.35 ± 0.06	0.416 ± 0.009	0.41 ± 0.03	0.4489 ± 0.0043	0.46 ± 0.02

*this work

[#]Certified values reported by Liang and Gregoire.[1]

[&1]Recommend values reported by Govindaraju.[2]

[&2]Recommend values reported by Wang et. al.[3]

[&3]Recommend values reported by Gu et. al.[4]

Table S-6 Measured results (N = 3) of REEs mass fractions in two basalt CRMs (BCR-2 and BHVO-2) using the MUN-ICP-MS. The measured values are the average from 3 measurements (n = 3) by MUN-ICP-MS with the uncertainties error bars defined as ± SD.

Element	BCR-2 (μg g^{-1})		BHVO-2 (μg g^{-1})	
	Measured*	Certified[#]	Measured*	Certified[#]
Sc	33.79 ± 0.34	33.53 ± 0.4	32.32 ± 0.17	31.83 ± 0.34
Y	35.87 ± 0.24	36.07 ± 0.37	25.75 ± 0.33	25.91 ± 0.28
La	25.32 ± 0.39	25.08 ± 0.16	15.43 ± 0.16	15.2 ± 0.08
Ce	53.49 ± 0.27	53.12 ± 0.33	37.55 ± 0.14	37.53 ± 0.19
Pr	6.764 ± 0.041	6.827 ± 0.044	5.360 ± 0.077	5.339 ± 0.028
Nd	28.84 ± 0.48	28.26 ± 0.37	24.34 ± 0.28	24.27 ± 0.25
Sm	6.540 ± 0.121	6.547 ± 0.047	6.045 ± 0.058	6.032 ± 0.057
Eu	2.036 ± 0.030	1.989 ± 0.024	2.077 ± 0.020	2.043 ± 0.012
Gd	6.732 ± 0.040	6.811 ± 0.078	6.375 ± 0.024	6.207 ± 0.038
Tb	1.070 ± 0.025	1.077 ± 0.026	0.9378 ± 0.0069	0.9392 ± 0.006
Dy	6.404 ± 0.047	6.424 ± 0.055	5.313 ± 0.025	5.280 ± 0.028
Ho	1.329 ± 0.029	1.313 ± 0.011	0.9818 ± 0.0086	0.9887 ± 0.0053
Er	3.636 ± 0.018	3.670 ± 0.038	2.550 ± 0.036	2.511 ± 0.014
Tm	0.5396 ± 0.0073	0.5341 ± 0.006	0.3378 ± 0.0059	0.3349 ± 0.0031
Yb	3.3619 ± 0.0289	3.392 ± 0.036	1.987 ± 0.007	1.994 ± 0.027
Lu	0.5115 ± 0.0042	0.5049 ± 0.0078	0.2702 ± 0.0026	0.2754 ± 0.0024

*this work

[#]Certified values reported by Jochum et. al.[5]

References

1. Q. Liang and D. C. Gregoire, Determination of trace elements in twenty six Chinese geochemistry reference materials by inductively coupled plasma-mass spectrometry, *Geostand. Geoanal. Res.*, 2000, **24**, 51-63.
2. K. Govindaraju, 1994 compilation of working values and sample description for 383 geostandards, *Geostand. Geoanal. Res.*, 1994, **18**, 1-158.
3. C. S. Wang, T. X. Gu, Q. H. Chi, W. D. Yan and M. C. Yan, New series of rock and sediment geochemical reference materials, *Geostand. Geoanal. Res.*, 2001, **25**, 145-152.
4. T. X. Gu, W. D. Yan, C. Y. Shi, M. C. Yan and W. Bo, New series of soil geochemical reference materials (GSS 10-16) from the main overburden region in China, *Geostand. Geoanal. Res.*, 2003, **27**, 197-202.
5. K. P. Jochum, U. Weis, B. Schwager, B. Stoll, S. A. Wilson, G. H. Haug, M. O. Andreae and J. Enzweiler, Reference values following ISO guidelines for frequently requested rock reference materials, *Geostand. Geoanal. Res.*, 2016, **40**, 333-350.